

RESEARCH

Open Access



# Identification and enrichment of potential pathways in the buffy coat of patients with DRE using non-targeted metabolomics integrated with GEO Datasets

Hailin Zhu<sup>2,3</sup>, Suyue Zheng<sup>4</sup>, Liyuan Xie<sup>1</sup>, Yi Yun<sup>5</sup>, Patrick Kwan<sup>3</sup>, Ben Rollo<sup>3</sup> and Hui Huang<sup>1\*</sup>

## Abstract

**Background** This study aims to identify potential biomarkers in the buffy coat of drug-resistant epilepsy (DRE) patients with mesial temporal lobe epilepsy and to elucidate associated pathways.

**Methods** A comprehensive non-targeted metabolomic and Gene Expression Omnibus (GEO) datasets analysis was first performed on buffy coat from DRE patients and non-epilepsy (CON) patients. Potential enriched biomarkers and pathways were integrated with gene expression profiles from GEO datasets to identify robust biomarkers.

**Results** In the DRE group, there were 15 patients (10 males and 5 females), with an average age of  $(37.67 \pm 15.53)$  years. In the CON group, there were 10 patients (7 males and 3 females), with an average age of  $(51.60 \pm 18.20)$  years. A total of 27 potential biomarkers were identified, including 7 down-regulated and 8 up-regulated. Additionally, 9 potential pathways related to DRE were identified. Notably, purine metabolism, tryptophan metabolism and aminoacyl-tRNA metabolism were closely related to DRE. Purine metabolism was up-regulated, while aminoacyl-tRNA and tryptophan metabolism were down-regulated.

**Conclusions** The integration of metabolomic data with GEO datasets analysis offers a new strategy to identify robust biomarkers and pathways. The findings obtained from the buffy coat analysis offer potential insights for the diagnosis and treatment of DRE.

**Keywords** Non-targeted metabolomics, Pathways, Bioinformatics, Drug resistant epilepsy

## Introduction

As one of the most common neurological disorders, epilepsy is estimated to affect around 70 million people worldwide [1]. Although the number of available antiseizure medications (ASMs) has increased substantially in the past three decades, about 30% of patients continue to experience seizures despite treatment, categorizing them as having drug-resistant epilepsy (DRE) [2]. Mesial temporal lobe epilepsy (mTLE) is among the most common forms of adult focal epilepsy and is frequently drug resistant [3]. While some patients with mTLE may be candidates for resective surgery,

\*Correspondence:

Hui Huang  
[huanghui0714@vip.sina.com](mailto:huanghui0714@vip.sina.com)

<sup>1</sup> Department of Neurosurgery, the Second Affiliated Hospital of Nanchang University, 566 Xuefu Road, Nanchang 330000, China

<sup>2</sup> School of Pharmacy, Nanchang University, Nanchang, China

<sup>3</sup> Department of Neuroscience, School of Translational Medicine, Monash University, Melbourne, Australia

<sup>4</sup> Department of Neurosurgery, the First Affiliated Hospital of Nanchang University, Nanchang, China

<sup>5</sup> Biobank Center, the Second Affiliated Hospital of Nanchang University, Nanchang, China



© The Author(s) 2025. **Open Access** This article is licensed under a Creative Commons Attribution-NonCommercial-NoDerivatives 4.0 International License, which permits any non-commercial use, sharing, distribution and reproduction in any medium or format, as long as you give appropriate credit to the original author(s) and the source, provide a link to the Creative Commons licence, and indicate if you modified the licensed material. You do not have permission under this licence to share adapted material derived from this article or parts of it. The images or other third party material in this article are included in the article's Creative Commons licence, unless indicated otherwise in a credit line to the material. If material is not included in the article's Creative Commons licence and your intended use is not permitted by statutory regulation or exceeds the permitted use, you will need to obtain permission directly from the copyright holder. To view a copy of this licence, visit <http://creativecommons.org/licenses/by-nc-nd/4.0/>.

25–35% of mTLE patients fail to achieve sustained seizure freedom after surgery, often leading to cognitive and behavioral impairments [4]. Therefore, identifying potential biomarkers and the mechanisms underlying DRE patients with mTLE is crucial for improving epilepsy treatment.

Over the past decade, metabolomics has been extensively utilized in the fields of disease diagnosis, pathophysiological mechanism, and therapy [5]. Non-targeted metabolomics is a high-throughput technique that comprehensively and rapidly identify metabolites changes within organisms [6, 7]. However, extracting relevant disease pathways from this vast amount of data remains a challenge. Gene Expression Omnibus (GEO) datasets can complement metabolomics by providing insights into intricate disease mechanisms, improving the understanding of diseases as a whole [8].

In this study, as shown in Fig. 1, we integrate non-targeted metabolomics with bioinformatics to explore potential pathways of mTLE with DRE. Unlike previous non-targeted metabolomics studies in clinical epilepsy research [9], we conducted a metabolomics analysis of the buffy coat.

This study aims to perform a comprehensive analysis of the buffy coat in mTLE DRE patients and non-neurological disease patients. We hope that this study will offer new strategies and insights for the diagnosis and treatment of drug-resistant mesial temporal lobe epilepsy.

## Materials and methods

### Characteristics of the patients

mTLE patients were enrolled from the Second Affiliated Hospital of Nanchang University between January to December 2019. These patients had been taking more than two ASMs for over a year without achieving seizure freedom [10] and were classified into the drug-resistant group (DRE group). They were matched with 10 patients without neurological diseases, treated in our hospital during this period, and classified as the control group (CON group). For both the DRE group and the CON group, the exclusion criteria were (1) Patients with metabolic disorders. (2) Patients with other neurological diseases aside from epilepsy. (3) Patients with blood system-related diseases. (4) Patients who participated in other clinical trials or did not provide informed consent form.

### Acquisition and preparation of buffy coat

All participants avoided strenuous exercise and alcohol consumption for 24 h and did not eat or drink for 10 h before blood collection. The blood collection time was between 7 and 9 am.

In this study, 2 mL blood sample was collected from each participant through the venous blood sampling method, which was left to stand for half an hour. Following centrifugation at 12,000 rpm for 10 min, the sample was separated into three distinct layers, with the upper layer contained plasma, the middle layer contained buffy coat, and the lower layer contained red blood cells. We carefully removed the upper plasma layer and placed the buffy coat layer into a sterile test tube.

We pipetted 50  $\mu$ L of the preparation, and added 300  $\mu$ L of 20% acetonitrile aqueous solution, the mixture was vortexed for 3 min, followed by centrifugation at 12,000 rpm for 10 min at 4 °C. Then, 200  $\mu$ L of the supernatant was collected, left to stand at -20 °C for half an hour. And then centrifuged at 12,000 rpm for 3 min, pipetted 180  $\mu$ L of the sample, and injected it into the AB TripleTOF 6600 for further analysis.

### HPLC conditions and MS conditions

Each sample was analyzed using two different LC/MS methods. One aliquot was analyzed under positive ion mode and separated on the T3 column (Waters ACQUITY Premier HSS T3 Column 1.8  $\mu$ m, 2.1 mm \* 100 mm) with 0.1% formic acid in water as mobile phase A and 0.1% formic acid in acetonitrile as mobile phase B, following this gradient: the mobile phase B was increased from 5 to 20% over 2 min, then a rise to 60% in the next 3 min, followed by a rise to 99% in 1 min, which was maintained for 1.5 min. Finally, it returned to 5% mobile phase B within 0.1 min and was held for 2.4 min. The MS conditions were set as follows: column temperature at 40 °C, flow rate of 0.4 mL/min, injection volume of 6  $\mu$ L. The negative ion mode used the same elution gradient as the positive mode.

Data acquisition was performed in information-dependent acquisition mode with the use of Analyst TF Software (version 1.7.1, Sciex, Concord, ON, Canada). The source parameters were configured as follows: ion source gas 1 and ion source gas 2 at 50 psi; curtain gas at 25 psi, temperature set to 550 °C, declustering potential at 60 V or -60 V for positive or negative modes, respectively, and ion spray voltage floating at 5000 V or -4000 V for positive or negative modes, respectively. The TOF MS scan settings were set as follows: mass range of 50–1000 Da, accumulation time of 200 ms, and dynamic background enabled. The product ion scan parameters settings were set as follows: mass range of 25–1000 Da; accumulation time of 40 ms, collision energy of 30 V or -30 V for positive or negative modes, respectively, collision energy spread of 15. The resolution was set to UNIT, charge state to 1+, intensity to 100 cps, isotopes within 4 Da excluded, mass tolerance at 50 ppm,

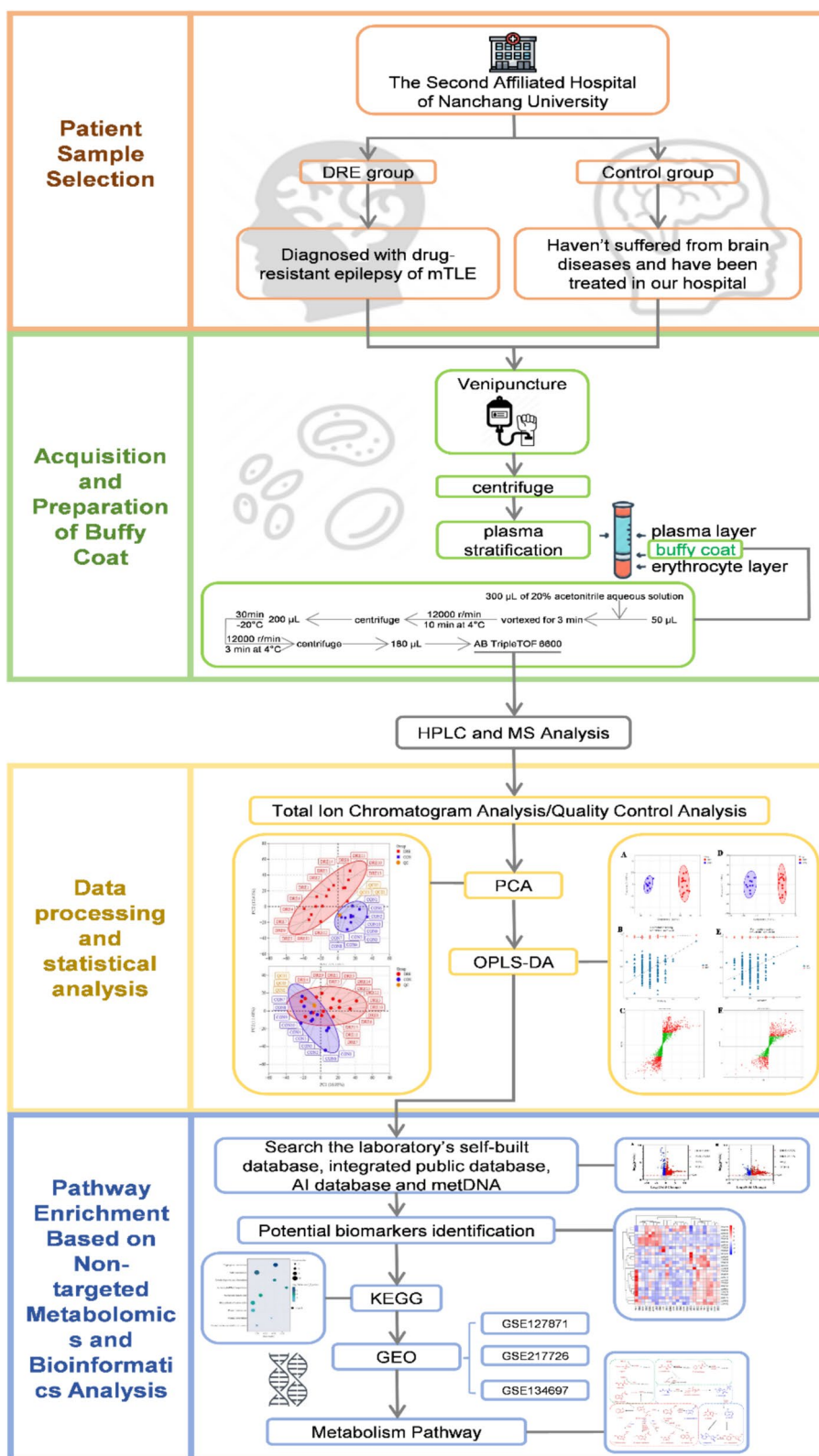


**Fig. 1** Flowchart of identifying biomarkers and potential pathways in vesicles from patients with drug-resistant mesial temporal lobe epilepsy based on untargeted metabolomics and bioinformatics analysis

and the maximum number of candidate ions to monitor per cycle was 18.

#### Data processing and statistical analyses

The raw data obtained from LC–MS was transformed into mzXML format using ProteoWizard software for subsequent data analysis. Peak extraction, alignment and retention time correction were both carried out using the XCMS program. The “SVR” approach was applied to adjust the peak parameters. Peaks with a detection rate  $\leq 50\%$  in any samples were excluded. Subsequently, potential biomarkers were identified by querying our laboratory’s database and publicly available databases.

The data were normalized to achieve unit variance and then unsupervised principal component analysis (PCA) was conducted in R ([www.r-project.org](http://www.r-project.org)). The results of hierarchical cluster analysis for potential biomarkers were displayed as heatmaps with accompanying dendrograms. Meanwhile, the Pearson correlation coefficients between each samples were computed using the `cor` function in R and shown as heatmaps only. Both hierarchical cluster analysis and Pearson correlation coefficients analyses were performed using the `ComplexHeatmap` package in R. The standardized potential biomarkers signal intensities results were displayed using a color spectrum.

For the two-group comparison, differential potential biomarkers were identified based on VIP ( $VIP > 1$ ) and  $p$ -value ( $p < 0.05$ , Student’s  $t$ -test). VIP values were obtained from the OPLS-DA results, which included score and permutation plots, and were visualized by the `MetaboAnalyst R` package. Prior to OPLS-DA analysis, the data underwent log transformation ( $\log_2$ ) and mean centering. To prevent overfitting, a permutation test with 200 iterations was carried out to ensure robustness.

Potential biomarkers were identified and subsequently mapped to the KEGG Pathway database by KEGG database (<http://www.kegg.jp/kegg/compound/>, <http://www.kegg.jp/kegg/pathway.html>, <https://cloud.metware.cn/>). Significantly enriched pathways were determined using a hypergeometric test’s  $p$ -value for the given set of potential biomarkers.

#### Pathway enrichment based on non-targeted metabolomics and bioinformatics analysis

Raw data were obtained from the Gene Expression Omnibus (GEO) database to enrich relevant genes based on specific criteria: (1) Samples must originate from human subjects. (2) Each group in the GEO dataset must contain more than three patients ( $n > 3$ ). (3) The focus is specifically on mesial temporal lobe epilepsy. Gene data from each dataset were analyzed using either GEO2R. Common differentially expressed genes across the datasets were identified, and these genes were

subsequently integrated with metabolomics data using `MetaboAnalyst 6.0`. This integration facilitated Joint Pathway Analysis to enrich potential metabolic pathways associated with the disease. Related pathways (integrated) were analyzed for enrichment using the Hypergeometric Test, with Degree Centrality as the topology measure and Combine queries as the integration method. Metabolic pathways with more than three potential biomarkers were selected and regarded as potential pathways, threshold was set arbitrarily and kept consistent across data sets. The selected enrichment results included the pathway.

## Results

### Characteristics of the patients

As shown in Tab. S1, the DRE group consisted of 15 patients (10 males), with a mean age of ( $37 \pm 15.53$ ) years. In most cases, unilateral interictal discharges were noted in the left hemisphere. The control group consisted of 10 patients (7 males), with a mean age of ( $51.6 \pm 18.2$ ) years.

### Total ion chromatogram analysis

As shown in Fig. S2–4, in order to evaluate the stability and accuracy of HPLC conditions and MS conditions, for every 10 samples, a quality control sample was prepared and subjected to quality control analysis. As shown in Fig. S2, the established detection method has of high stability and reliability. As shown in Fig. S3, there was no cross-contamination between samples. As shown in Fig. S5 and Tab. S2, the stability of the detection process and the experimental data were consistent and reliable.

### Principal component analysis

In order to obtain an initial understanding of the overall differences between metabolome sample groups and the magnitude of variation, PCA was performed. As shown in Fig. S5, regardless of whether in positive ion mode or negative ion mode, there was a separation trend between the DRE group and the CON group, and there are differences in the metabolome within the sample groups, with the quality control samples located centrally. This indicated that there was significant differences between the CON group and the DRE group for the potential biomarkers.

We detected ion pairs from each sample and developed a PCA model. Based on the PCA model, we also monitored the QC samples to verify the stability of the instrument. As shown in Fig. S6, each point represents a sample, and due to systematic errors in the instrument, the points exhibit fluctuations up and down. QC samples with PC1 scores within a range of plus or minus three standard deviations are considered to have good instrument stability.

### Orthogonal partial least squares discriminant analysis

While PCA provides a broad view of sample data, it may not be sensitive to some metabolites with minimal correlation. To address this, we performed OPLS-DA analysis, which amplifies the differences between CON and DRE groups, making it easier to identify potential potential biomarkers.

As shown in Fig. 2A, both the positive and negative spectrum conditions demonstrated clear separation between the CON and DRE groups, which was more distinct than that was observed in the PCA score plots. We also evaluated the predictive and explanatory probability of the OPLS-DA. As shown in Fig. 2B, the positive and negative spectra models both showed  $Q^2 > 0.5$  and  $Q^2 > R^2X$ , indicating that the OPLS-DA model we established had strong predictive ability. By performing 200 random permutation tests with OPLS-DA, the final result showed that  $p = 0.03 < 0.05$ , further confirming the reliability of the model. Furthermore, we developed S-plot, as shown in Fig. 2C, the points lower left corners and closer to the upper right represent significant differences between two groups. Red points represent metabolites with a  $VIP > 1$  and green points represent metabolites with a  $VIP \leq 1$ . Only metabolites with a  $VIP > 1$  were considered potential biomarkers.

### Potential biomarkers identification

As shown in Fig. S7, a total of 3,244 potential biomarkers were identified, comprising 457 up-regulated metabolites and 270 down-regulated metabolites. We further selected biomarkers with  $p < 0.05$  (Student's t-test) and  $VIP > 1$ . Under these conditions, as shown in Table 1, a total of 27 potential biomarkers were identified, comprising 7 down-regulated and 8 up-regulated potential biomarkers. As shown in Fig. 3A, to visualize the distribution and variation of these potential biomarker across different samples we constructed heatmaps..

### Potential biomarkers enrichment analysis and pathway analysis

We conducted KEGG pathway enrichment, as shown in Fig. 3B, where the dot size reflects the number of potential biomarkers enriched in the respective pathway, and the closer the P value is to 0, the more pronounced the enrichment effect. Finally, a total of 9 pathways potentially associated with drug-resistant epilepsy were identified.

### Potential pathway enrichment

To further enrich the metabolic pathways, an integrative analysis was conducted by processing data through MetaboAnalyst 6.0. As shown in 3C, this analysis

revealed a total of 9316 common significant genes across 3 GEO datasets (GSE127871, GSE217726 and GSE134697). By integrating this data with the potential biomarkers, we identified 84 potential metabolic pathways related to temporal lobe epilepsy (See supplementary). To enhance the reliability of the pathway analysis, only pathways enriched with more than three biomarkers were considered. Using this criteria, we found that three pathways were significantly enriched: purine metabolism, tryptophan metabolism, and aminoacyl-tRNA metabolism closely linked to the TLE and drug-resistant epilepsy.

### Discussion

This study specifically investigated changes of metabolites in the buffy coat, which is distinct from the more commonly used samples such as blood, urine, and cerebrospinal fluid samples in non-targeted metabolomics research in epilepsy. In fact, a total of 60% of studies typically used blood samples, including serum and plasma [9]. However, there is no report on the metabolomics of the buffy coat, which comprises platelets, lymphocytes, monocytes, and granulocytes. These metabolites are closely associated with immune cells and may play a role in mediating peripheral immune responses, which in turn interact with CNS immunity in epilepsy [11].

Our analysis of non-targeted metabolomic analysis was performed in patients with mTLE and drug-resistant epilepsy in this study, ultimately identifying 27 potential biomarkers from buffy coat. Further investigation into these potential biomarkers revealed that 7 of them are amino acids and derivatives (L-Lysine, Glutamine, L-Glutamic acid, Asparagine, Kynurenic acid, L-Phenylalanine, L-Tryptophan) and 3 are organic acids and derivatives (1,6-di-O-phosphono-beta-D-fructofuranose, (S)-2-acetamido-6-oxopimelic acid, 3-Isopropylmalic acid). These findings align with previous research from both animal and clinical studies, using different samples such as blood, urine and cerebrospinal fluid, where amino acids and organic acid derivatives were found to be potential biomarkers for epilepsy [9]. Our results indicate that the potential biomarkers identified from buffy coat may also be similar to traditional samples in influencing the development of DRE. As shown in Table 2, the orange cells represent potential biomarkers involved in pathways or there is literature related to potential biomarkers and epilepsy based on metabolomics or DRE. Based on a review of the available literature, it was found that 15 potential biomarkers have been documented to correlate with epilepsy, and 10 potential biomarkers have been implicated in both metabolomics and epilepsy [12–26].

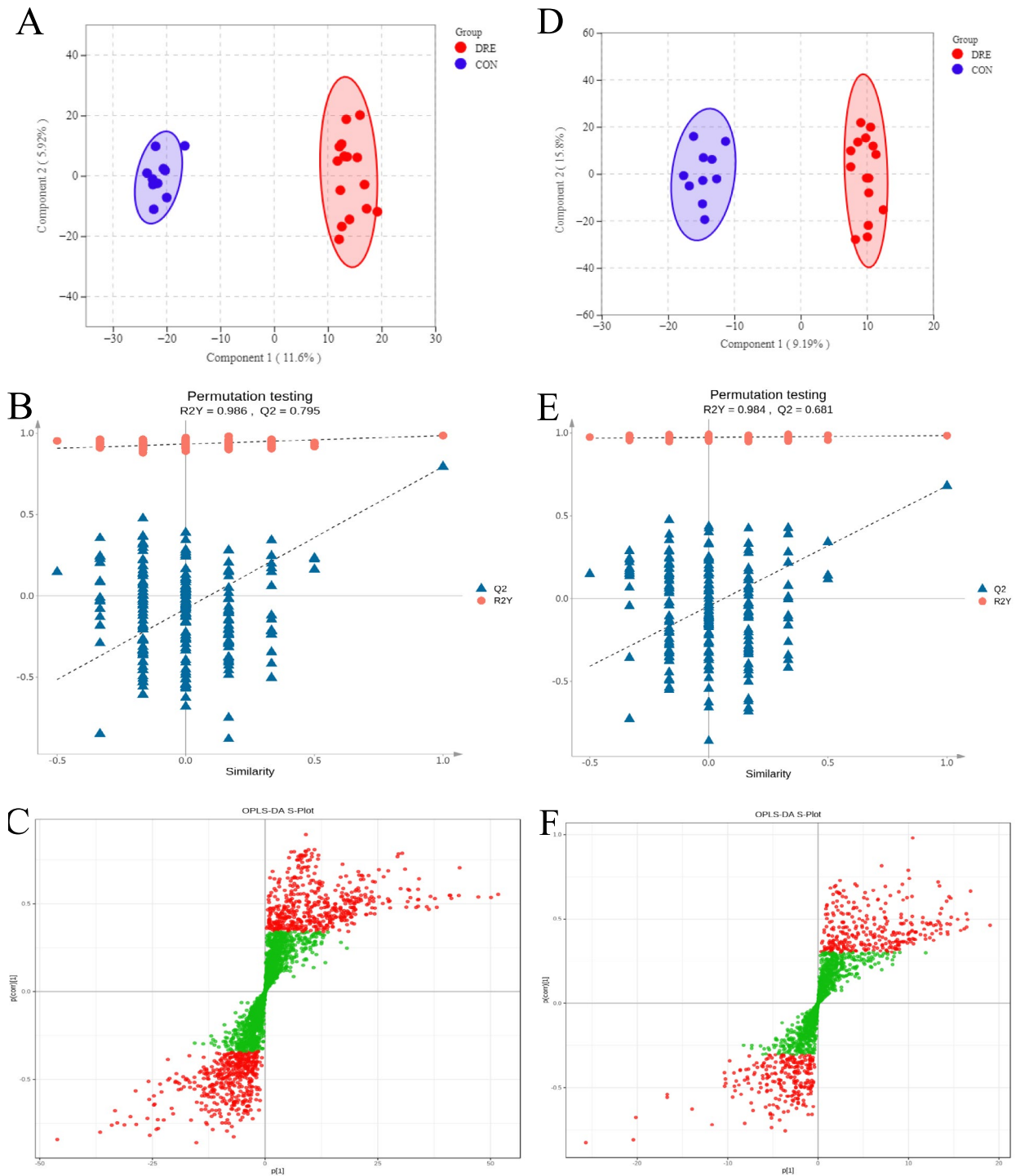


**Fig. 2** OPLS-DA models resulting from UPLC/Q-TOF-MS spectra. **A, D** represents, respectively, the OPLS-DA two-dimensional graph of the DRE group and the CON group (red dots represent the DRE group and blue dots represent the CON group); **B, E** represents the permutation test evaluation of OPLS-DA; **C, F** represent the s-plot of metabolites (red dots show  $VIP > 1$ , green dots show  $VIP \leq 1$ ); **A-C** represents the ESI+ mode; **D-F** represent the ESI- mode

**Table 1** Potential biomarkers identified from ESI<sup>+</sup> mode and ESI<sup>-</sup> mode

Num	Mode	Compounds	Formula	RT (min)	Cpd_ID	p	VIP
1	Negative	L-Lysine	C <sub>6</sub> H <sub>14</sub> N <sub>2</sub> O <sub>2</sub>	0.67	C00047	0.007	1.57
2	Negative	Glycinamide ribonucleotide	C <sub>7</sub> H <sub>15</sub> N <sub>2</sub> O <sub>8</sub> P	0.67	C03838	0.013	1.55
3	Positive	Glutamine	C <sub>5</sub> H <sub>10</sub> N <sub>2</sub> O <sub>3</sub>	0.79	C00064	0.019	1.37
4	Negative	N-Acetyl-D-glucosamine	C <sub>8</sub> H <sub>15</sub> NO <sub>6</sub>	0.81	C00140	0.044	1.36
5	Negative	1,6-di-O-phosphono-beta-D-fructofuranose	C <sub>6</sub> H <sub>14</sub> O <sub>12</sub> P <sub>2</sub>	0.83	C05378	0.013	1.50
6	Positive	L-Glutamic acid	C <sub>5</sub> H <sub>9</sub> NO <sub>4</sub>	0.86	C00025	0.044	1.15
7	Negative	Asparagine	C <sub>4</sub> H <sub>8</sub> N <sub>2</sub> O <sub>3</sub>	1.19	C00152	0.016	1.63
8	Negative	Inosinic acid	C <sub>10</sub> H <sub>13</sub> N <sub>4</sub> O <sub>8</sub> P	1.19	C00130	0.008	1.75
9	Negative	Xanthine	C <sub>5</sub> H <sub>4</sub> N <sub>4</sub> O <sub>2</sub>	1.25	C00385	0.012	1.41
10	Negative	2'-Deoxyadenosine	C <sub>10</sub> H <sub>13</sub> N <sub>5</sub> O <sub>3</sub>	1.30	C00559	0.006	1.66
11	Positive	(S)-2-acetamido-6-oxopimelic acid	C <sub>9</sub> H <sub>13</sub> NO <sub>6</sub>	1.38	C05539	0.040	1.19
12	Positive	Kynurenic acid	C <sub>10</sub> H <sub>7</sub> NO <sub>3</sub>	1.44	C01717	0.033	1.18
13	Negative	2'-Deoxyinosine	C <sub>10</sub> H <sub>12</sub> N <sub>4</sub> O <sub>4</sub>	1.79	C05512	0.003	1.95
14	Negative	D-Allose	C <sub>6</sub> H <sub>12</sub> O <sub>6</sub>	1.96	C01487	0.006	1.86
15	Positive	2'-Deoxyuridine	C <sub>9</sub> H <sub>12</sub> N <sub>2</sub> O <sub>5</sub>	1.97	C00526	0.047	1.39
16	Positive	3-Isopropylmalic acid	C <sub>7</sub> H <sub>12</sub> O <sub>5</sub>	1.97	C04411	0.000	1.84
17	Positive	L-Phenylalanine	C <sub>9</sub> H <sub>11</sub> NO <sub>2</sub>	1.97	C00079	0.001	1.99
18	Negative	Tryptamine	C <sub>10</sub> H <sub>12</sub> N <sub>2</sub>	2.34	C00398	0.004	1.93
19	Negative	Indole-3-acetamide	C <sub>10</sub> H <sub>10</sub> N <sub>2</sub> O	2.34	C02693	0.016	1.64
20	Positive	L-Tryptophan	C <sub>11</sub> H <sub>12</sub> N <sub>2</sub> O <sub>2</sub>	2.37	C00078	0.002	1.92
21	Positive	Indole	C <sub>8</sub> H <sub>7</sub> N	2.37	C00463	0.013	1.50
22	Positive	5-Methoxyindoleacetate	C <sub>11</sub> H <sub>11</sub> NO <sub>3</sub>	2.37	C05660	0.001	1.99
23	Positive	N-Acetylserotonin	C <sub>12</sub> H <sub>14</sub> N <sub>2</sub> O <sub>2</sub>	2.37	C00978	0.007	1.74
24	Negative	Adenine	C <sub>5</sub> H <sub>5</sub> N <sub>5</sub>	2.38	C00147	0.002	2.20
25	Positive	Biotin	C <sub>10</sub> H <sub>16</sub> N <sub>2</sub> O <sub>3</sub> S	2.41	C00120	0.022	1.56
26	Positive	Indoleacetaldehyde	C <sub>10</sub> H <sub>9</sub> NO	2.60	C00637	0.016	1.34
27	Positive	N-Methylserotonin	C <sub>11</sub> H <sub>14</sub> N <sub>2</sub> O	3.05	C06212	0.005	1.69

Importantly, three potential biomarkers have been associated with drug-resistant epilepsy (DRE). Notably, potential biomarkers Glutamine, Asparagine, and Kynurenic acid may represent robust biomarkers for diagnosed DRE. Biomarkers N-Acetyl-D-glucosamine, Inosinic acid, Xanthine, N-Acetylserotonin, and Biotin are being identified for the first time in metabolomics studies related to DRE, which could be due to the use of the buffy coat samples in this study. These findings suggest that the buffy coat provides valuable insights into the localized metabolic changes associated with DRE, offering an innovative and sensitive method for diagnosing the condition. After enriching potential biomarkers through KEGG analysis, a total of 9 pathways were enriched (tryptophan metabolism, ABC transporters, protein digestion and absorption, aminoacyl-tRNA metabolism and purine metabolism, nucleotide metabolism, biosynthesis of amino acids, purine metabolism, mineral absorption and central carbon metabolism in cancer). Further analysis with the GEO dataset revealed a potential association between

drug-resistant temporal lobe epilepsy and the pathways of purine metabolism, aminoacyl-tRNA metabolism and tryptophan metabolism. It is worth noting that although ABC transporters were not among the final enrichment potential pathways, the increased expression of efflux transporters in the blood-brain barrier (BBB), primarily from the ATP-binding cassette (ABC) superfamily, contribute to the limited penetration of ASMs into the brain, thus affecting the occurrence of drug-resistant epilepsy [27].

As shown in Fig. 4, Glycinamide ribonucleotide (GAR) is downregulated, while glutamine and inosinic acid (IMP) are significantly upregulated in the DRE group. This suggests that the downregulation of the PPAT gene in the DRE group, as found in the GEO datasets analysis (GSE127871, GSE134697, and GSE217726), leads to early inhibition of purine synthesis. However, the availability of glutamine as an amino donor could compensate for and promote the synthesis of IMP, subsequently enhancing purine synthesis in DRE [28]. Additionally, the increase in IMP and the decrease in 2'-deoxyadenosine suggest

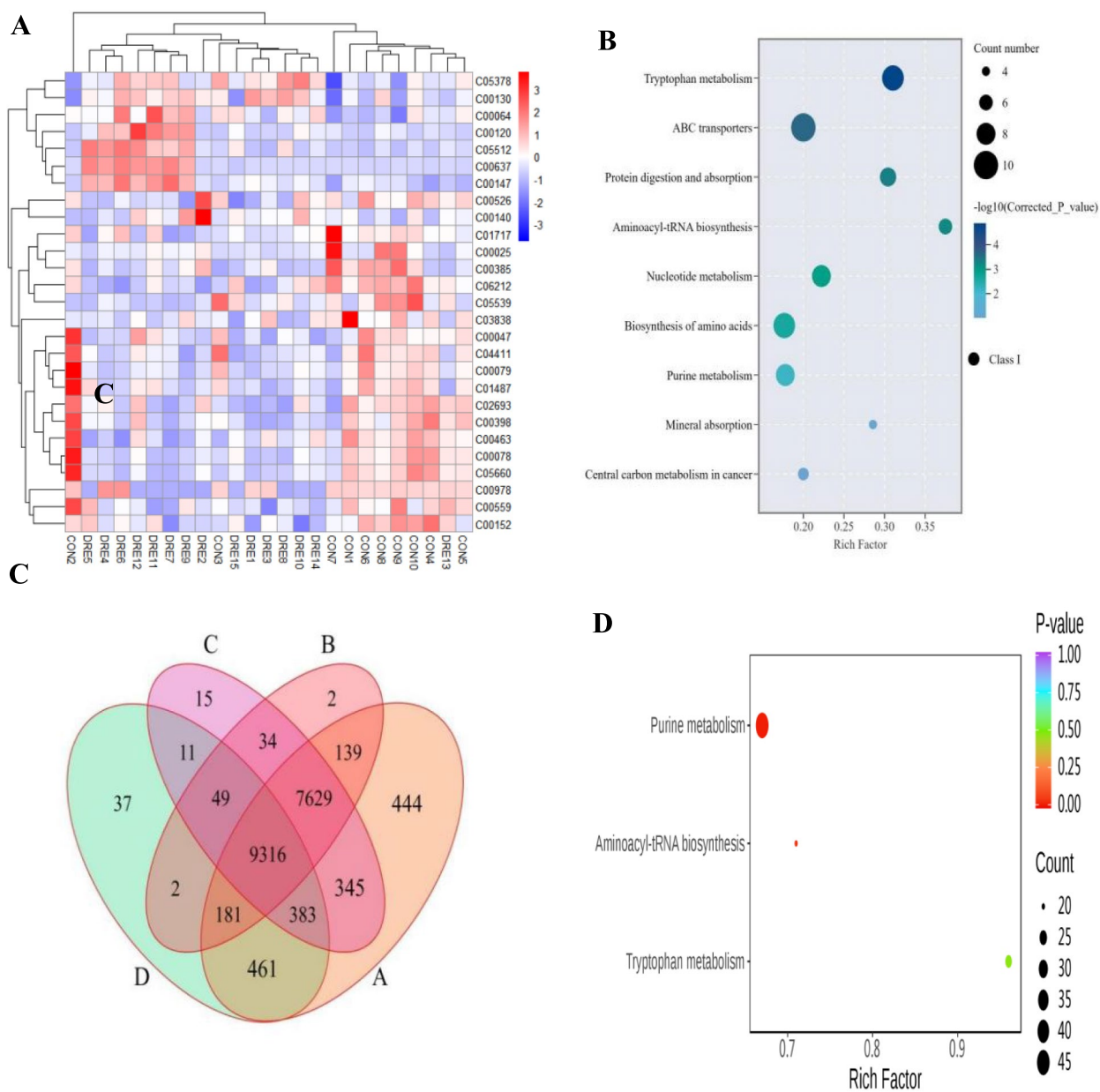


**Fig. 3** Potential pathways enrichment. **A** Heatmaps of potential biomarkers; **B** KEGG pathway enrichment; **C** Venn diagram of common genes from bioinformatics analysis; **D** Potential pathways identified after integrated analysis of metabolomics and bioinformatics analysis

a restricted conversion between AMP and IMP, and between ATP and 2'-deoxyadenosine, thereby limiting the breakdown metabolism of 2'-deoxyadenosine and promoting the utilization of IMP. The decrease in xanthine in the DRE group indicates an impairment in the breakdown process of purine metabolism, which may further impact the metabolism of uric acid. High levels of uric acid are considered to be associated with the mechanisms of epilepsy onset and medication use [29],

although it is unclear if this is due to epilepsy itself or the result of ASM treatment [30]. Although there are higher average levels of uric acid in the DRE patients compared to the control patients, the variability within the DRE group was considerable. The upregulation of inosinic acid, adenine, and 2'-deoxyinosine involves the recycling of nucleotides in purine metabolism, suggesting that cells in the DRE group may enhance nucleic acid repair or respond to increased cellular stress. It is now recognized

**Table 2** Potential biomarkers involved in pathways and literature

Markers	Epilepsy	Metabolomics	DRE	Tryptophan metabolism	ABC transporters	Aminoacyl-tRNA biosynthesis	Purine metabolism	Biosynthesis of amino acids	Ref.
1									[12]
2									
3									[13, 14]
4									[15]
5									
6									[16]
7									[17, 18]
8									[19]
9									[19]
10									
11									
12									[20]
13									
14									
15									
16									
17									[21]
18									[22]
19									
20									[23]
21									[20]
22									
23									[24]
24									[25]
25									[26]
26									
27									

that purines affect seizures, and that ketogenic diets and purine metabolites like adenosine, when used in the treatment of DRE, can increase the sensitivity or activity levels of adenosine receptors [31, 32]. Overall, in the DRE group, there is an enhancement in purine metabolism and an inhibition in degradation, this dysregulation could potentially affect the roles of ATP and adenosine in DRE. As ATP and adenosine metabolites were not measured in

this experiment, the relationship remains to be further analyzed.

In addition, aminoacyl-tRNA metabolism is suppressed in the DRE group (Fig. S8). In this study, potential biomarkers including L-Lysine L-Glutamic acid, Asparagine, L-Phenylalanine, and L-Tryptophan showed downregulation in the DRE group. These amino acids are involved in neurotransmitter synthesis,

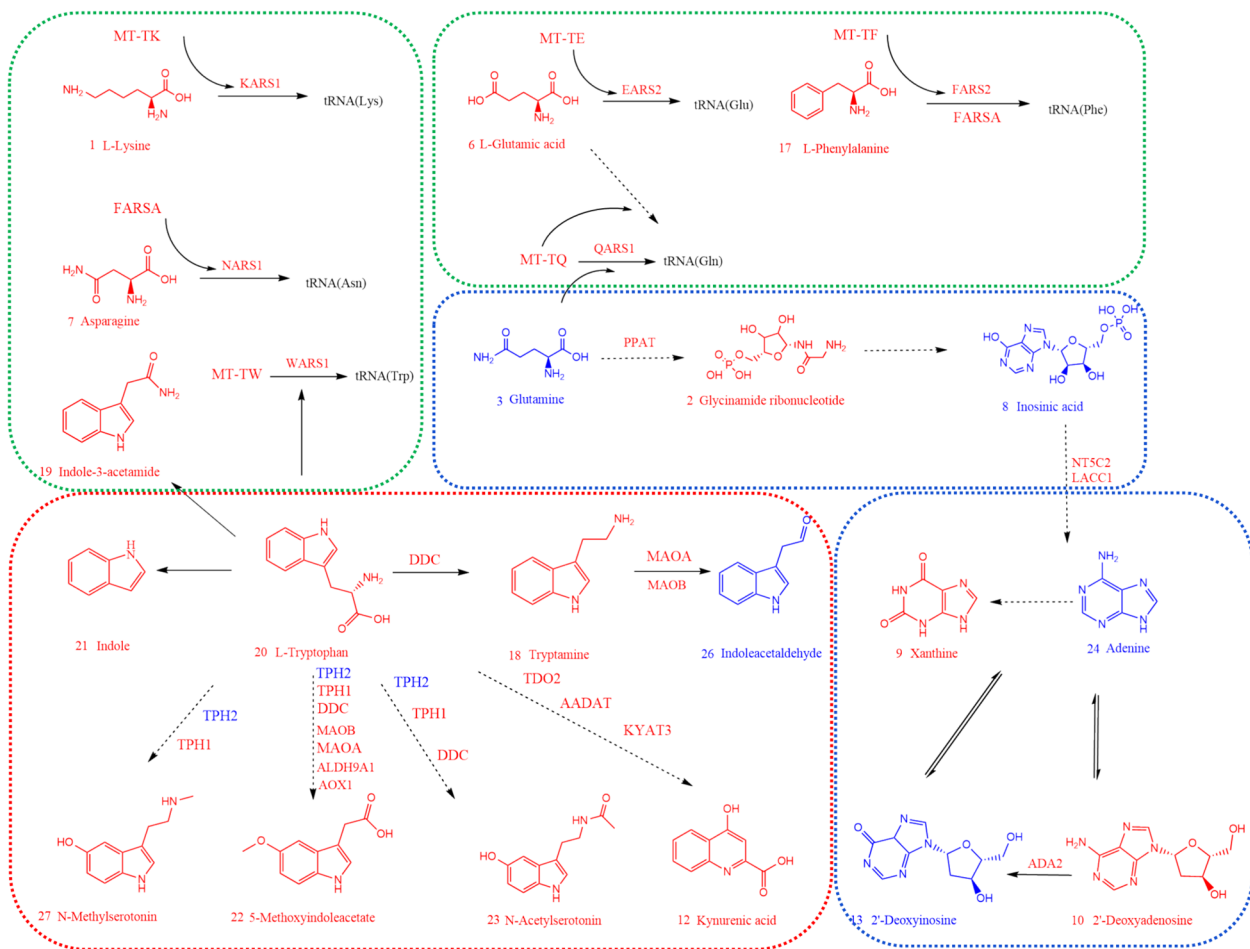


**Fig. 4** Enriched pathways and relevant potential biomarkers involved in this study. The dotted arrows mean multiple steps and the solid arrows mean one step between two potential biomarkers. Red potential markers indicate higher concentrations in the control group compared to the DRE group. Blue potential markers indicate higher concentrations in the DRE group compared to the control group. Different colored boxes represent different pathways

potentially impacting the occurrence of drug-resistant epilepsy [18]. GEO dataset analysis revealed a consistent downregulation of mitochondrial tRNA-associated genes, such as MT-TK, MT-TE, MT-TN, MT-TE, and MT-TW in the DRE group. Mutations in these genes are linked to mitochondrial syndromes and have been reported in association with Refractory Status Epilepticus [33, 34]. The genes KARS1, EARS2, NARS, FARS2, FARS1, and WARS1, which load the respective amino acids into their corresponding tRNAs, constitute the essential first step in protein translation. Analysis of GEO data showed a downregulation of these genes in the epilepsy group, and the report showed that mutations in these genes lead to neurological developmental anomalies [35]. Aminoacyl-tRNA metabolism was found to inhibit protein synthesis and disrupt mitochondrial energy metabolism, influencing the development of DRE.

Tryptophan metabolism is also overall inhibited in the DRE group. Tryptophan metabolism is the pathway most closely related to epilepsy among the three pathways [36, 37]. However, this is the first study that has implicated the tryptophan metabolism pathway in DRE through non-targeted metabolomics. Tryptophan is the only precursor for the biosynthesis of serotonin. As shown in Fig. 4, the levels of serotonin metabolites (N-Acetylserotonin, N-Methylserotonin, 5-Methoxyindoleacetate) were significantly reduced in the DRE group, but there is no obvious difference in serotonin levels between the DRE and CON patients, possibly because peripheral serotonin cannot cross the blood-brain barrier [38]. Approximately 90% of tryptophan is oxidized into kynurenine, the metabolic products of tryptophan, such as kynurenic acid, which has been shown to be significantly downregulated in DRE ( $p < 0.05$ ) [39]. Tryptophan is metabolized into indole derivatives by microbes such

as *Clostridium* sp., *Bacteroides* sp., and *Escherichia coli* [40, 41]. Tryptamine, indole-3-acetamide, and indole are also downregulated in the DRE group. Analysis of GEO datasets in bioinformatics reveals that the genes involved in tryptophan metabolism, including DDC, MAOA, MAOB, ALDH9A1, AOX1, and KYAT3, are significantly downregulated. Overall, these findings point to the potential role of tryptophan metabolism is inhibited in the DRE. Further studies are required to validate the biomarkers and pathways involved in this study, especially those that have not been previously linked to DRE.

### Summary

This study presents the first metabolomic analysis of the buffy coat in drug-resistant epilepsy, identifying 27 potential biomarkers. The integration of non-targeted metabolomics with available GEO datasets provides insights into the mechanisms of DRE, highlighting the pathways of purine metabolism, tryptophan metabolism, and aminoacyl-tRNA metabolism. These results provide a foundation for both biomarker discovery, and to enhance our understanding of the mechanisms of mTLE and drug-resistant epilepsy. Further studies are required to validate the biomarkers and pathways involved in this study, especially those have never been reported related to epilepsy.

### Abbreviations

CON	Non-epilepsy patients
DRE	Drug-resistant epilepsy
ASMs	Antiseizure medications
GEO	Gene Expression Omnibus
PCA	Principal Component Analysis
OPLS-DA	Orthogonal Partial Least Squares Discriminant Analysis

### Supplementary Information

The online version contains supplementary material available at <https://doi.org/10.1186/s40001-025-02609-0>.

Additional file 1.

### Acknowledgements

Thanks to all the volunteers for their generous donation of samples.

### Author contributions

HL Zhu wrote the original draft, SY Zheng prepared data curation and analysis, LY Xie conducted the investigation and data collection, Y Yun collected samples and stored them, P Kwan wrote, reviewed and edited, and supervised, B Rollo drafted and revised, and H Huang conducted the methodology and supervision.

### Funding

This work was supported by the Jiangxi Provincial Natural Science Foundation (20242BAB20460, 20242BAB25470), Jiangxi Provincial Health Commission science and technology grant (202110051, 202130350) and Jiangxi Province Administration of Traditional Chinese Medicine Science and Technology Plan (2017A265, 2024B0262). Science and Technology Research Project of Jiangxi

Provincial Department of Education (170089), Hailin Zhu (202208360118) and Hui Huang (202308360151) were supported by the China Scholarship Council as exchange scholars.

### Data availability

No datasets were generated or analysed during the current study.

### Declarations

#### Ethics approval and consent to participate

The Ethics Committee of the Second Affiliated Hospital of Nanchang University granted approval for this project.

#### Informed consent

Informed consent was obtained from all subjects involved in the study.

#### Competing interests

The authors declare no competing interests.

Received: 22 January 2025 Accepted: 16 April 2025

Published online: 26 April 2025

### References

- Sander JWAS, Shorvon SD. Epidemiology of the epilepsies. *J Neurol Neurosurg Psychiatry*. 1996;61:433–43. <https://doi.org/10.1136/jnnp.61.5.433>.
- Moshe SL, Perucca E, Ryvlin P, et al. Epilepsy: new advances. *Lancet*. 2015;385:884–98. [https://doi.org/10.1016/S0140-6736\(14\)60456-6](https://doi.org/10.1016/S0140-6736(14)60456-6).
- Ren E, Curia G. Synaptic reshaping and neuronal outcomes in the temporal lobe epilepsy. *Int J Mol Sci*. 2021;22:3860. <https://doi.org/10.3390/ijms22083860>.
- Mills JD, Van Vliet EA, Chen BJ, et al. Coding and non-coding transcriptome of mesial temporal lobe epilepsy: critical role of small non-coding RNAs. *Neurobiol Dis*. 2020;134: 104612. <https://doi.org/10.1016/j.nbd.2019.104612>.
- Tian H, Ni Z, Lam SM, et al. Precise metabolomics reveals a diversity of aging-associated metabolic features. *Small Methods*. 2022;6: e2200130. <https://doi.org/10.1002/smt.202200130>.
- Nicholson JK, Lindon JC, Holmes E. "Metabonomics": understanding the metabolic responses of living systems to pathophysiological stimuli via multivariate statistical analysis of biological NMR spectroscopic data. *Xenobiotica*. 1999;29(11):1181–9. <https://doi.org/10.1080/004982599238047>.
- Weckwerth W, Morgenthal K. Metabolomics: from pattern recognition to biological interpretation. *Drug Discov Today*. 2005;10(22):1551–8. [https://doi.org/10.1016/S1359-6446\(05\)03609-3](https://doi.org/10.1016/S1359-6446(05)03609-3).
- Hu X, Ni S, Zhao K, et al. Bioinformatics-led discovery of osteoarthritis biomarkers and inflammatory infiltrates. *Front Immunol*. 2022;13: 871008. <https://doi.org/10.3389/fimmu.2022.871008>.
- Lai WL, Du D, Chen L. Metabolomics provides novel insights into epilepsy diagnosis and treatment: a review. *Neurochem Res*. 2022;47:844–59. <https://doi.org/10.1007/s11064-021-03510-y>.
- Kwan P, Arzimanoglou A, Berg AT, et al. Definition of drug resistant epilepsy: consensus proposal by the ad hoc task force of the ILAE commission on therapeutic strategies. *Epilepsia*. 2010;51(6):1069–77. <https://doi.org/10.1111/j.1528-1167.2009.02397.x>.
- Mu XP, Zhang XC, Gao HH, et al. Crosstalk between peripheral and the brain-resident immune components in epilepsy. *J Integr Neurosci*. 2022;21(1):1–12. <https://doi.org/10.31083/jjin2101009>.
- Engelke UF, Van Outersterp RE, Merx J, et al. Untargeted metabolomics and infrared ion spectroscopy identify biomarkers for pyridoxine-dependent epilepsy. *J Clin Invest*. 2021;131(15): e148272. <https://doi.org/10.1172/JCI148272>.

13. Dynka D, Kowalcze K, Paziewska A. The role of ketogenic diet in the treatment of neurological diseases. *Nutrients*. 2022;14(23):5003. <https://doi.org/10.3390/nu14235003>.
14. Detour J, Bund C, Behr C, et al. Metabolomic characterization of human hippocampus from drug-resistant epilepsy with mesial temporal seizure. *Epilepsia*. 2018;59:607–16. <https://doi.org/10.1111/epi.14000>.
15. Sun RC, Young LEA, Bruntz RC, et al. Brain glycogen serves as a critical glucosamine cache required for protein glycosylation. *Cell Metab*. 2021;33:1404–17. <https://doi.org/10.1016/j.cmet.2021.05.003>.
16. Miljanovic N, Van Dijk RM, Buchecker V, et al. Metabolomic signature of the Dravet syndrome: a genetic mouse model study. *Epilepsia*. 2021;62:2000–14. <https://doi.org/10.1111/epi.16976>.
17. Zhao X, Cheng PX, Xu R, et al. Insights into the development of pentylentetrazole-induced epileptic seizures from dynamic metabolomic changes. *Metab Brain Dis*. 2022;37:2441–55. <https://doi.org/10.1007/s11011-022-01018-0>.
18. Altintas M, Yildirim M, Ucar CI, et al. Ketogenic diet-responsive drug-resistant epilepsy in a case of asparagine synthetase deficiency with a novel compound heterozygous missense variant. *Clin Neurol Neurosurg*. 2023;230: 107772. <https://doi.org/10.1016/j.clineuro.2023.107772>.
19. Beamer E, Lacey A, Alves M, et al. Elevated blood purine levels as a biomarker of seizures and epilepsy. *Epilepsia*. 2021;62:817–28. <https://doi.org/10.1111/epi.16839>.
20. Peng Y, Chiu ATG, Li VWY, et al. The role of the gut-microbiome-brain axis in metabolic remodeling amongst children with cerebral palsy and epilepsy. *Front Neurol*. 2023;14:1109469. <https://doi.org/10.3389/fneur.2023.1109469>.
21. Zhu HL, Wu ZY, Yu YZ, et al. Integrated non-targeted metabolomics and network pharmacology to reveal the mechanisms of berberine in the long-term treatment of PTZ-induced epilepsy. *Life Sci*. 2024;336: 122347. <https://doi.org/10.1016/j.lfs.2023.122347>.
22. Paley EL, Perry G, Sokolova O. Tryptamine induces axonopathy and mitochondriopathy mimicking neurodegenerative diseases via tryptophanyl-tRNA deficiency. *Curr Alzheimer Res*. 2024;10(9):987–1004. <https://doi.org/10.2174/15672050113106660164>.
23. Skiba A, Pellegata D, Morozova V, et al. Pharmacometabolic effects of pteryxin and valproate on pentylentetrazole-induced seizures in zebrafish reveal vagus nerve stimulation. *Cells*. 2023;12:1540. <https://doi.org/10.3390/cells12111540>.
24. Lima E, Cabral FR, Cavalheiro EA, et al. Melatonin administration after pilocarpine-induced status epilepticus: a new way to prevent or attenuate postlesion epilepsy? *Epilepsy Behav*. 2011;20:607–12. <https://doi.org/10.1016/j.yebeh.2011.01.018>.
25. Brister D, Werner BA, Gideon G, et al. Central nervous system metabolism in autism, epilepsy and developmental delays: a cerebrospinal fluid analysis. *Metabolites*. 2022;12(5):371. <https://doi.org/10.3390/metab12050371>.
26. Yuasa M, Matsui T, Ando S, et al. Consumption of a low-carbohydrate and high-fat diet (the ketogenic diet) exaggerates biotin deficiency in mice. *Nutrition*. 2013;29:1266–70. <https://doi.org/10.1016/j.nut.2013.04.011>.
27. Leandro K, Bicker J, Alves G, et al. ABC transporters in drug-resistant epilepsy: mechanisms of upregulation and therapeutic approaches. *Pharmacol Res*. 2019;144:357–76. <https://doi.org/10.1016/j.phrs.2019.04.031>.
28. Abdullah MO, Zeng RX, Margerum CL, et al. Mitochondrial hyperfusion via metabolic sensing of regulatory amino acids. *Cell Rep*. 2022;40: 111198. <https://doi.org/10.1016/j.celrep.2022.111198>.
29. Park KI, Hwang S, Son H, et al. Prognostication in epilepsy with integrated analysis of blood parameters and clinical data. *J Clin Med*. 2024;13:5517. <https://doi.org/10.3390/jcm13185517>.
30. Daniels SD, Boison D. Bipolar mania and epilepsy pathophysiology and treatment may converge in purine metabolism: a new perspective on available evidence. *Neuropharmacology*. 2023;241: 109756. <https://doi.org/10.1016/j.neuropharm.2023.109756>.
31. Weltha L, Reemmer J, Boison D. The role of adenosine in epilepsy. *Brain Res Bull*. 2019;151:46–54. <https://doi.org/10.1016/j.brainresbull.2018.11.008>.
32. Ruskin DN, Kawamura M Jr, Masino SA. Adenosine and ketogenic treatments. *J Caffeine Adenosine Res*. 2020;10(3):104–9. <https://doi.org/10.1089/caff.2020.0011>.
33. Indelicato E, Pfeilstetter J, Zech M, et al. New-onset refractory status epilepticus due to a novel MT-TF variant: time for acute genetic testing before treatment? *Neurol Genet*. 2023;9(2): e200063. <https://doi.org/10.1212/nxg.000000000200063>.
34. Duan H, Pan C, Wu T, et al. MT-TN mutations lead to progressive mitochondrial encephalopathy and promotes mitophagy. *Biochim Biophys Acta Mol Basis Dis*. 2024;1870: 167043. <https://doi.org/10.1016/j.bbdis.2024.167043>.
35. Manole A, Efthymiou S, O'Connor E. De novo and bi-allelic pathogenic variants in NARS1 cause neurodevelopmental delay due to toxic gain-of-function and partial loss-of-function effects. *Am J Hum Genet*. 2020;107:311–24. [https://doi.org/10.1212/wnl.96.15\\_supplement.4714](https://doi.org/10.1212/wnl.96.15_supplement.4714).
36. Żarnowska I, Wróbel-Dudzińska D, Tulidowicz-Bielak M, et al. Changes in tryptophan and kynurenine pathway metabolites in the blood of children treated with ketogenic diet for refractory epilepsy. *Seizure*. 2019;69:265–72. <https://doi.org/10.1016/j.seizure.2019.05.006>.
37. Dey S, Dubey V, Dixit AB, et al. Differential levels of tryptophan-kynurenine pathway metabolites in the hippocampus, anterior temporal lobe, and neocortex in an animal model of temporal lobe epilepsy. *Cells*. 2022;11:3560. <https://doi.org/10.3390/cells11223560>.
38. Agus A, Planchais J, Sokol H. Gut microbiota regulation of tryptophan metabolism in health and disease. *Cell Host Microbe*. 2018;23:716–24. <https://doi.org/10.1016/j.chom.2018.05.003>.
39. Cervenka I, Agudelo LZ, Ruas JL. Kynurenines: Tryptophan's metabolites in exercise, inflammation, and mental health. *Science*. 2017;357(369):9794. <https://doi.org/10.1126/science.aaf9794>.
40. Lee JH, Lee J. Indole as an intercellular signal in microbial communities. *FEMS Microbiol Rev*. 2010;34:426–44. <https://doi.org/10.1111/j.1574-6976.2009.00204.x>.
41. Smith EA, Macfarlane GT. Enumeration of human colonic bacteria producing phenolic and indolic compounds: effects of pH, carbohydrate availability and retention time on dissimilatory aromatic amino acid metabolism. *J Appl Bacteriol*. 1996;81:288–302. <https://doi.org/10.1111/j.1365-2672.1996.tb04331.x>.

## Publisher's Note

Springer Nature remains neutral with regard to jurisdictional claims in published maps and institutional affiliations.